Level densities in ^{56,57}Fe and ^{96,97}Mo

A. Schiller,[1,*] E. Algin,[1,2,3,4] L. A. Bernstein,[1] P. E. Garrett,[1] M. Guttormsen,[5] M. Hjorth-Jensen,[5] C. W. Johnson,[6] G. E. Mitchell,[2,3] J. Rekstad,[5] S. Siem,[5] A. Voinov,[7] and W. Younes[1]

[1]*Lawrence Livermore National Laboratory, L-414, 7000 East Avenue, Livermore, California 94551, USA*

[2]*North Carolina State University, Raleigh, North Carolina 27695, USA*

[3]*Triangle Universities Nuclear Laboratory, Durham, North Carolina 27708, USA*

[4]*Department of Physics, Osmangazi University, Meselik, Eskisehir 26480, Turkey*

[5]*Department of Physics, University of Oslo, N-0316 Oslo, Norway*

[6]*San Diego State University, San Diego, California 92182, USA*

[7]*Frank Laboratory of Neutron Physics, Joint Institute of Nuclear Research, 141980 Dubna, Moscow region, Russia*

(Received 24 February 2003; revised manuscript received 10 June 2003; published 26 November 2003)

Level densities up close to the neutron binding energy have been extracted from primary γ spectra for ^{56,57}Fe and ^{96,97}Mo nuclei using (^{3}He, $\alpha\gamma$) and (^{3}He, ^{3}He$'\gamma$) reactions on ^{57}Fe and ^{97}Mo targets. It is shown that statistical spectroscopy provides a useful tool in this mass region. Apparent step structures in the level-density curves are tentatively explained by a schematic microscopic model comprising single-particle level spacings and seniority-conserving and seniority-nonconserving interactions.

DOI: 10.1103/PhysRevC.68.054326 PACS number(s): 21.10.Ma, 25.55.Hp, 27.40.+z, 27.60.+j

The group at the Oslo Cyclotron Laboratory (OCL) has recently developed a new method (the so-called Oslo method) to extract the level density and radiative strength function from primary γ spectra [1]. The method can be characterized as a further development of the sequential extraction method [2,3]. The Oslo method has been extensively tested in the rare-earth mass region which has led to many fruitful applications [4–7]. However, whether this approach could be extended to much lighter nuclei or to nuclei near closed shells was an open question. The first extension of the Oslo method outside the rare-earth region was to ^{27,28}Si [8]. For these nuclei a direct comparison was possible between the average of the tabulated discrete levels and the level density determined via the Oslo method. The overall agreement for the level density obtained via these two methods was excellent. This surprising agreement in such light nuclei encouraged us to test the method in intermediate nuclei. In such nuclei the level density is sufficiently low that a purely statistical analysis may not be appropriate, but the level density is sufficiently high that direct counting methods fail. We chose to test the method on ^{56,57}Fe and ^{96,97}Mo.

The ^{56}Fe nucleus was especially chosen due to astrophysical interest in this isotope. Partition functions of nuclei in this mass region, i.e., the Laplace transforms of their level densities, determine both the relative nuclear abundances in the late-time presupernova star [9] and the high-temperature weak rates [10] which again govern the mass of the homologous core in core-collapse supernovae. The nucleus ^{96}Mo is of special interest in the investigation of the $|N-Z|$ dependence of level densities, since the mass 96 isobars are the only ones in the nuclear chart where one can find three different stable nuclei with $|N-Z|$ varying by eight units from ^{96}Zr to ^{96}Ru. Also the $|N-Z|$ dependence of level densities can have significant astrophysical importance [11], since many reactions take place on unstable isotopes and therefore most of their reaction cross sections must be estimated by Hauser-Feshbach-type calculations [12,13].

The purpose of the present work is to investigate the validity of the Oslo method in an intermediate mass region, to report on experimental level densities of ^{56,57}Fe and ^{96,97}Mo nuclei, and to provide a schematic explanation of the observed step structures in these curves.

The experiments were performed at the MC-35 cyclotron at the OCL using a ~2-nA beam of 45-MeV ^{3}He particles. The self-supporting targets were isotopically enriched to 94.7% and 94.2% and had thicknesses of 3.4 mg/cm^2 and 2.1 mg/cm^2 for ^{57}Fe and ^{97}Mo, respectively. Each experiment ran for ~5 days, and about 200,000 relevant particle-γ coincidences were recorded in each analyzed reaction channel. The charged ejectiles were identified and their energies were measured in a ring of eight collimated Si ΔE-E telescopes placed at 45° with respect to the beam direction. The thicknesses of the front and end detectors were 140 and 3000 μm, respectively, and shielding against δ electrons was achieved with a 19-μm-thick Al foil. The distance from the target was 5 cm, giving a total solid angle coverage of 0.3% of 4π, and the energy resolution was ~0.3 MeV over the entire spectrum. The γ rays were detected in 28 collimated $5'' \times 5''$ NaI(Tl) detectors collectively called CACTUS [14] surrounding the target and particle detectors. The total efficiency of CACTUS was ~15% of 4π and the resolution was ~6% of the deposited energy at 1.3 MeV. In addition, one 60% Ge (high purity) detector was used in the setup to monitor the selectivity and populated spin distribution of the reactions. Raw α-particle data are shown in Fig. 1 for the case of the ^{97}Mo(^{3}He, α)^{96}Mo reaction, where discrete transfer peaks are observed up to ~6 MeV in excitation energy indicating the opening of the neutron $g_{9/2}$ shell.

From the known Q value and the reaction kinematics, the ejectile energy can be transformed into initial excitation en-

*Electronic address: schiller@nscl.msu.edu

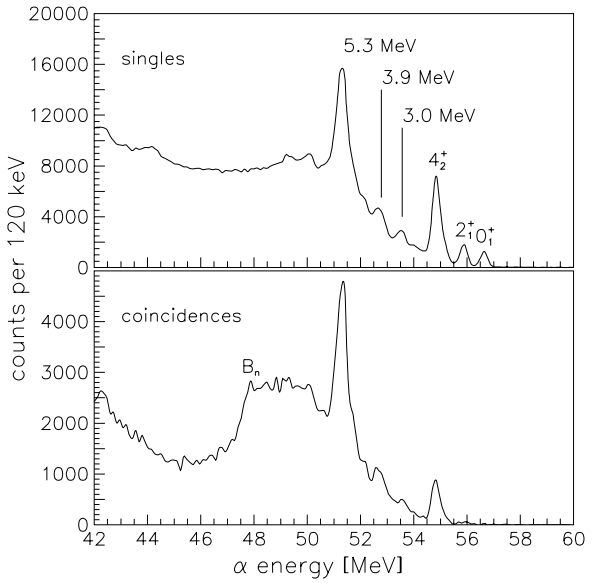

FIG. 1. Singles α spectrum (upper panel) and α-γ coincidence spectrum (lower panel) for the ^{97}Mo(^{3}He, α)^{96}Mo reaction. At the neutron binding energy B_n, the coincidence spectrum shows a rapid decrease reflecting the lower γ multiplicity in the decay from low-lying states in ^{95}Mo which are populated by neutron emission. The transfer peaks to the first three states are well known from the (p, d) reaction [15]. The strong transfer peak at 5.3 MeV has not been observed previously, and presumably indicates the opening of the $g_{9/2}$ shell at this energy.

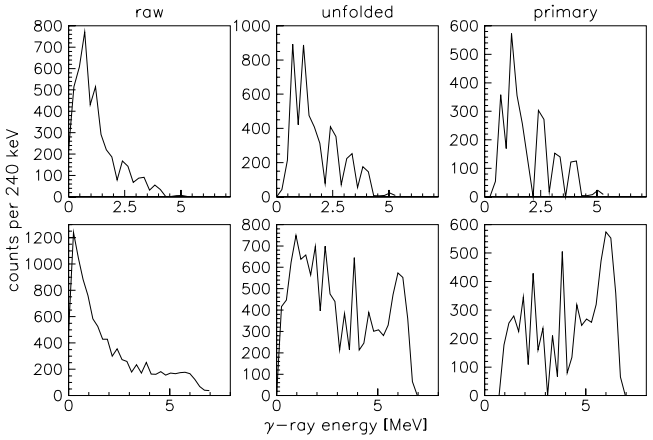

FIG. 2. Raw, unfolded, and primary γ spectra from the ^{57}Fe(^{3}He, $\alpha\gamma$)^{56}Fe reaction at 5-MeV excitation energy (upper panels) and from the ^{57}Fe(^{3}He, ^{3}He$'\gamma$)^{57}Fe reaction at 6.2-MeV excitation energy (lower panels).

ergy of the residual nuclei. Using the particle-γ coincidence technique, each γ ray can be assigned to a cascade depopulating a certain initial excitation energy in the residual nucleus. The data are therefore sorted into total γ-ray spectra originating from different initial excitation energy bins. Every spectrum is then unfolded using a Compton-subtraction method which preserves the fluctuations in the original spectra and does not introduce further, spurious fluctuations [16]. From the unfolded spectra, a primary γ matrix is constructed using the subtraction method of Ref. [17]. The basic assumption behind this method is that the γ-ray decay pattern from any excitation energy bin is independent of whether states in this bin are populated directly via the (^{3}He, α) or (^{3}He, ^{3}He$'$) reactions or indirectly via γ decay from higher excited levels following the initial nuclear reaction. This assumption is trivially fulfilled if one populates the same levels with the same weights within any excitation energy bin, since the decay branchings are properties of the levels and do not depend on the population mechanisms. On the other hand, if one populates, e.g., vastly different spin distributions within one excitation energy bin via the two different population mechanisms, the γ-decay patterns should be different as well. As an example of the data analysis discussed in this paragraph, the raw, unfolded, and primary γ spectra are shown for the ^{57}Fe(^{3}He, $\alpha\gamma$)^{56}Fe and ^{57}Fe(^{3}He, ^{3}He$'\gamma$)^{57}Fe reactions in Fig. 2.

Finally, the primary γ matrix is factorized using the generalized Brink-Axel hypothesis [18,19]. The original hypothesis states that the giant dipole resonance (GDR) can be built on every excited state, and that the properties of the GDR do not depend on the temperature of the nuclear state on which it is built. This hypothesis can be generalized to include not only the GDR but any type of nuclear excitation and results in the assumption that primary γ spectra originating from the excitation energy E can be factorized into a γ-ray transmission coefficient $\mathcal{T}(E_\gamma)$, which depends only on the γ-transition energy E_γ, and into the level density $\rho(E-E_\gamma)$ at the final energy. This simple picture is complicated by the experimental fact that the Brink-Axel hypothesis is violated at sufficiently high temperatures ($\gtrsim$1–2 MeV). Especially, the width of the GDR has been shown to depend on temperature [20]. Models based on Fermi-liquid theory suggest a T^2 dependence for this effect [21,22]. Within the rather low excitation-energy range under study in the present work, however, the temperature dependence of the γ-ray transmission coefficient is not so well established experimentally. For the purpose of this work, we assume therefore that (i) temperature changes weakly within our experimentally accessible excitation energy range (roughly $T\propto\sqrt{E}$) and (ii) variations of the γ-ray transmission coefficient with temperature are small (roughly a second-order effect in T according to Ref. [21]). Within these assumptions we can expect to replace the actual temperature dependence in $\mathcal{T}(E_\gamma, T)$ by a constant, average value $\langle T\rangle$ of the temperature and, thus, recover the applicability of the generalized Brink-Axel hypothesis. The systematic error we introduce by this approximation is largest for the low-energy part ($\lesssim$2–3 MeV) of the γ-ray transmission coefficient where it can reach $\sim$20%.

The factorization of the primary γ matrix into $\mathcal{T}(E_\gamma)$ and $\rho(E-E_\gamma)$ is determined by a least-χ^2 fit to the primary γ matrix, using no *a priori* assumptions about the functional form of either the level density or the γ-ray transmission coefficient [1]. In the present work, the error estimate of the first-generation matrix has been improved over [1], thereby decreasing spurious fluctuations in the resulting level densities and γ-ray transmission coefficients. An example to illustrate the quality of the fit is shown in Fig. 3, where for the ^{97}Mo(^{3}He, ^{3}He$'\gamma$)^{97}Mo reaction we compare the experimental primary γ spectra from two different initial excitation

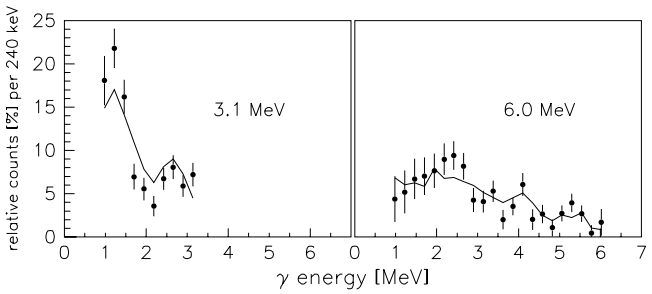

FIG. 3. Experimental primary γ spectra (data points with error bars) at two different initial excitation energies (indicated in the figure) compared to the least-χ^2 fit (solid lines) for the ^{97}Mo(^{3}He, ^{3}He$'\gamma$)^{97}Mo reaction. The fit is performed simultaneously to the entire primary γ matrix of which the two displayed spectra are only a small fraction. The first-generation spectra are normalized to one at each excitation energy bin.

energies to the least-χ^2 fit. Unfortunately, the mathematical structure of the relevant equations in the least-χ^2 fit does not allow us to find a unique solution for the level density and γ-ray transmission coefficient. However, it has been shown that all solutions with the same χ^2 can be obtained by the transformation of one randomly chosen solution according to [1]

$$\tilde{\rho}(E-E_\gamma) = A\,\exp[\alpha(E-E_\gamma)]\rho(E-E_\gamma), \tag{1}$$

$$\tilde{\mathcal{T}}(E_\gamma) = B\,\exp(\alpha E_\gamma)\mathcal{T}(E_\gamma). \tag{2}$$

The three free parameters A, B, and α have to be determined to give the physically most relevant solution to the least-χ^2 fit using independent experimental information. The most common way is to count the number of discrete levels at low excitation energies [23] and to use the average neutron resonance spacing at B_n to find values for A and α. The remaining parameter B is then determined using the average total radiative width of neutron resonances [6]. In the case of ^{56}Fe, there are no data on neutron resonances and, thus, the information about the level density around B_n in ^{56}Fe has to be obtained by different means. In order to do so, we calculate the level density at B_n in ^{57}Fe using a backshifted Fermi-gas expression with the parametrization of von Egidy *et al.* [24], where we apply an additional overall renormalization factor to match the level density determined from neutron resonance spacings. Then, we use the same level-density parametrization (including the same renormalization factor but with parameters appropriate for ^{56}Fe) to calculate the level density at B_n in ^{56}Fe. Using this data point instead of the unknown average neutron resonance spacing, we proceed in the same way as for the other three nuclei [1,25]. The estimated level density of ^{56}Fe at B_n obtained in this manner is in good agreement with experimental data obtained from particle evaporation studies [26].

In Fig. 4 we show the extracted level densities in ^{56,57}Fe and ^{96,97}Mo from the present data. The quality of the results strongly suggests that statistical methods can be applied in this intermediate mass region. This is further supported by, e.g., studies of the total γ cascade after keV-neutron capture where it has been shown that sufficient averaging over initial states allows the description of the resulting γ spectrum within the statistical model [27]. Since the experimental evidence strongly implies that the Oslo method can provide valid results in this intermediate mass region, we focus on the physics implications of the experimental level densities.

The most striking features in the level-density curves in Fig. 4 are the steps starting at 2.9 MeV in ^{56}Fe and 1.8 MeV

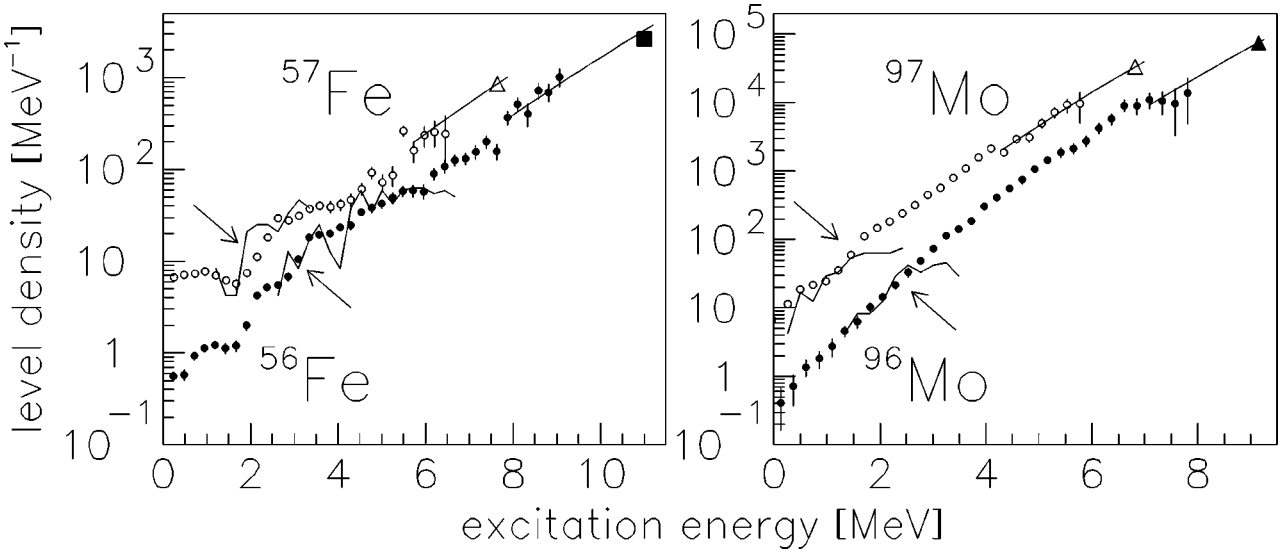

FIG. 4. Experimental level densities for the four nuclei under study (full and open symbols represent even and odd nuclei, respectively). Wherever available, level-density data from neutron resonance spacings have been added (triangles). The square represents level-density data from a particle evaporation study [26]. The smooth solid curves are the renormalized level-density parametrizations according to von Egidy *et al.* [24]. The jagged solid lines are level-density information from counting of discrete levels as given in the Table of Isotopes [23]. Apparent step structures in the level densities are marked by arrows. In the level density of ^{56}Fe, the bump and the plateau at 0.8 MeV and 2.0 MeV, respectively, are due to the first and second excited states.

in ^{57}Fe. These steps are verified in the level-density curves obtained from the counting of discrete levels. However, there are fluctuations due to the binning procedure, and the energy at which the discrete level scheme becomes incomplete (due to missing levels) is not known. As a result, evidence for step structures from discrete level schemes must be only provisional. The combination of these two independent data sets provides much stronger evidence. There is also a less pronounced, but still statistically significant, step structure at 1.2 MeV in ^{97}Mo. This structure cannot be observed from counting of discrete states; it is too high in energy and the level density is too large.[1] (A possible step structure in ^{96}Mo at 2.0 MeV is probably too smeared out in the present experimental data but might still be visible in the discrete level scheme.) It has been established in the rare-earth region that such low-lying step structures are connected to the breaking of the first nucleon Cooper pair [29]. It is therefore reasonable to assume that the same is true for lighter mass regions. The additional step at 6 MeV in the level-density curve of ^{96}Mo may be due to the opening of the $g_{9/2}$ shell which should occur at this excitation energy (see Fig. 1). A future systematic investigation of the Mo nuclei may shed more light on this issue. The structures in the level density data of the Fe nuclei at high excitation energies presumably reflect fluctuations due to poorer statistics.

The difference in binding energy between the even and odd systems is a measure for pairing correlation and can be calculated from the three-mass indicator of Dobaczewski *et al.* [30]. This indicator yields 1.3 MeV and 1.1 MeV for the Fe and Mo nuclei, respectively, which agrees well with the differences in excitation energy for the first steps in the level-density curves. Thus, the steps in neighboring nuclei appear at the same "effective" excitation energy, i.e., the excitation energy corrected for the contribution to the binding energy due to neutron-pairing correlations. Further, the proton pairing energies are 0.7 MeV and 1.0 MeV for the ^{57}Fe and ^{97}Mo nuclei, respectively. These energies should now correspond to the excitation energies of the steps in the two odd nuclei. However, the steps are delayed in excitation energy by 1.1 MeV and 0.2 MeV for these two nuclei. This might be explained by the fact that one not only has to invest the energy to break a proton Cooper pair but also at least one of the unpaired protons has to be promoted to the next unoccupied single-particle level. The average spacing of these levels can also be calculated using the Dobaczewski three-mass indicator, giving 1.9 MeV and 1.3 MeV in the two cases. Clearly, the higher single-particle spacing for ^{56}Fe as compared to ^{97}Mo leads to a larger delay in excitation energy for the appearance of the step structure. However, the exact excitation energy cannot be estimated from binding energies, since it will depend on the exact location of the Fermi energy within the single-particle level scheme.

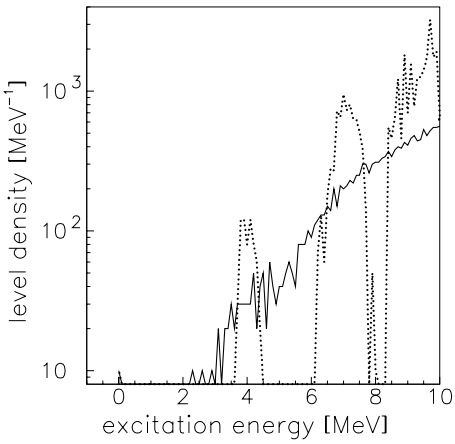

FIG. 5. Level density as a function of excitation energy. Model calculation (dotted line) using the Hamiltonian of Eq. (3) with ϵ =0.25 MeV, G=0.5 MeV, and $\kappa \approx 0$ MeV . Adding a random two-body interaction with the strength κ=0.14 MeV (solid line) results in a step structure similar to what is seen in the experimental level-density curve of the iron nuclei.

Another complication might arise from the effect of seniority-nonconserving interactions, which mix configurations of different seniority and smooth out the step structures in the level densities.[2] To investigate this, we have performed a model calculation. In the model we assume a system of eight particles scattered into an equidistant single-particle level scheme with eight doubly degenerate levels. As residual interactions we consider a pairing interaction and a seniority-nonconserving interaction. Thus, the model Hamiltonian is written as

$$\hat{H} = \epsilon \sum_{i=1}^{8} i a_i^\dagger a_i - \frac{1}{2} G \sum_{i,j=1}^{8} a_i^\dagger a_{\bar{i}}^\dagger a_{\bar{j}} a_j - \frac{1}{2} \kappa \sum_{i,j,k,l=1}^{8} W_{ijkl} a_i^\dagger a_j^\dagger a_k a_l, \tag{3}$$

where $a^\dagger$ and a are Fermion creation and annihilation operators and the labels with bars stand for time reversed orbits. The single-particle level spacing ϵ, the strength G of the pairing interaction, and the strength κ of the seniority-nonconserving interaction W are the only macroscopic parameters of the model. This model with good seniority, i.e., the case of κ=0, has already been diagonalized in Ref. [32], and the dotted line in Fig. 5 gives the distribution of eigenvalues with excitation energy, i.e., the exact level density of the model. The individual bumps contain mainly levels with the same seniority, thus the step structures in the level density can be explained by the

[1] It is worth noting that the counting of discrete levels provides an approximately complete level density only up to a level density value of about 60 levels per MeV in the four nuclei under study. This value can be extended using high-resolution γ detectors and the measurement of γ excitation functions from neutron inelastic scattering. However, even for the best investigated nucleus thus far – ^{112}Cd (see Ref. [28]) this value has been extended only to 160 levels per MeV. Even this best case would not be sufficient to perform complete spectroscopy up to the particle separation energy for any of the four nuclei measured in the present experiment.

[2] The effect of pairing correlations on the nuclear level density (mostly utilizing the concept of a nuclear temperature) has been investigated by numerous authors in the past, the first being Sano and Yamasaki [31]. In this work, however, we chose an entirely microscopic approach.

consecutive breaking of nucleon Cooper pairs. However, the experimental data show that in general the steps are much smoother than in such a simple model calculation indicating the need for seniority-nonconserving terms in the Hamiltonian.

An important contribution to seniority breaking comes from quadrupole collectivity, which can change rapidly with mass number for the nuclei under study. Strong, residual quadrupole-quadrupole interactions can lead to deformation of the nucleus and to a modification of the single-particle level spacing. Unfortunately, our simple model cannot incorporate a realistic quadrupole-quadrupole interaction; the smoothing of the level density, however, should not depend too much on the details of the seniority-nonconserving residual interaction. We choose therefore to model the quadrupole-quadrupole interaction by a random two-body interaction [33] of roughly equivalent strength where all the pairinglike terms have been set to zero, i.e., the W_{ijkl} in Eq. (3) are Gaussian random numbers of mean zero and width equal to one, except for the cases of $j=\bar{\imath}$ and $k=\bar{l}$ where $W_{i\bar{i}l\bar{l}}=0$.

Since in this more general case Eq. (3) does not have good seniority, exact diagonalization of the model Hamiltonian has to be performed within the full model space which is computationally very demanding, as one requires *all* levels, not just the lowest. For eight particles in eight doubly degenerate states there are 12 870 states (counting all magnetic substates). The number of levels (not counting magnetic substates) equals the number of states with spin projection $J_z=0$, thus yielding 4900 levels. For the present calculations, we used $\epsilon=0.25$ MeV, $G=0.5$ MeV, and $\kappa \approx 0$ MeV (pure pairing) and $\kappa=0.14$ MeV (pairing+random interaction). In Fig. 5, we show the resulting level densities of the two calculations. The resolved bumps with definite seniority in the pure pairing case are smeared out by the random interaction. The gaps between the bumps are rapidly being filled, while the bumps themselves are degraded into a step structure quite similar to the step structure seen in the experimental level-density curves of the iron nuclei. The occurrence of the step structure in the calculation is actually quite sensitive to the exact choice of the strength of the random interaction. A weak random interaction ($\kappa \leqslant 0.1$ MeV) does not fill the gaps between the bumps, a much stronger random interaction ($\kappa \geqslant 0.2$ MeV) produces a more smeared-out step structure in the level-density curve similar to the Mo data, indicating the presence of relatively stronger seniority-nonconserving interactions in the Mo nuclei. The range of values that produces good qualitative agreement with the Fe data is about 0.13 MeV $\leqslant \kappa \leqslant$ 0.16 MeV. However, due to the simplicity of the model, no attempt has been made to achieve quantitative agreement between the model and the experimental data.

In conclusion, we have shown that statistical methods such as the Oslo method can be applied to an intermediate mass region where the level density is still relatively low. New experimental data on level densities below B_n in ^{56,57}Fe and ^{96,97}Mo have been presented. Step structures in the level-density curves have been tentatively related to the breaking of nucleon Cooper pairs. The position of the step structures in energy depends on the exact location of the Fermi energy in the single-particle level scheme. The smoothness of the step structures depends on the strength of the seniority-nonconserving interactions, e.g., the quadrupole-quadrupole interaction relative to the pairing interaction and the average single-particle level spacing. The more pronounced step structures in the level density data of Fe compared to Mo indicate relatively stronger seniority-nonconserving interactions in the latter case. Our schematic calculations where random two-body interactions were used to model residual seniority-nonconserving interactions show that the low-energy part of theoretical level-density curves are very sensitive to the relative strengths of the different terms in the model Hamiltonian. The present experimental data therefore suggest a new approach for possible theoretical investigations of the pairing and quadrupole-quadrupole interactions.

Part of this work was performed under the auspices of the U.S. Department of Energy by the University of California, Lawrence Livermore National Laboratory under Contract No. W-7405-ENG-48. Financial support from the Norwegian Research Council (NFR) is gratefully acknowledged. G.M. acknowledges support by a U.S. Department of Energy Grant No. DE-FG02-97-ER41042. A.S. would like to thank Jason Pruet for interesting discussions.

[1] A. Schiller, L. Bergholt, M. Guttormsen, E. Melby, J. Rekstad, and S. Siem, Nucl. Instrum. Methods Phys. Res. A **447**, 498 (2000).
[2] G. A. Bartholomew, I. Bergqvist, E. D. Earle, and A. J. Ferguson, Can. J. Phys. **48**, 687 (1970).
[3] G. A. Bartholomew, E. D. Earle, A. J. Ferguson, J. W. Knowles, and M. A. Lone, Adv. Nucl. Phys. **7**, 229 (1973).
[4] A. Schiller, A. Bjerve, M. Guttormsen, M. Hjorth-Jensen, F. Ingebretsen, E. Melby, S. Messelt, J. Rekstad, S. Siem, and S. W. Ødegård, Phys. Rev. C **63**, 021306(R) (2001).
[5] E. Melby, M. Guttormsen, J. Rekstad, A. Schiller, S. Siem, and A. Voinov, Phys. Rev. C **63**, 044309 (2001).
[6] A. Voinov, M. Guttormsen, E. Melby, J. Rekstad, A. Schiller, and S. Siem, Phys. Rev. C **63**, 044313 (2001).
[7] S. Siem, M. Guttormsen, K. Ingeberg, E. Melby, J. Rekstad, A. Schiller, and A. Voinov, Phys. Rev. C **65**, 044318 (2002).
[8] M. Guttormsen, E. Melby, J. Rekstad, S. Siem, A. Schiller, T. Lönnroth, and A. Voinov, J. Phys. G **29**, 263 (2003).
[9] H. A. Bethe, G. E. Brown, J. Applegate, and J. M. Lattimer, Nucl. Phys. **A324**, 487 (1979).
[10] G. M. Fuller, W. A. Fowler, and M. J. Newman, Astrophys. J. **252**, 715 (1982).
[11] S. I. Al-Quraishi, S. M. Grimes, T. N. Massey, and D. A. Resler, Phys. Rev. C **63**, 065803 (2001).
[12] W. Hauser and H. Feshbach, Phys. Rev. **87**, 366 (1952).
[13] C. Angulo *et al.*, Nucl. Phys. **A656**, 3 (1999).

[14] M. Guttormsen, A. Atac, G. Løvhøiden, S. Messelt, T. Ramsøy, J. Rekstad, T. F. Thorsteinsen, T. S. Tveter, and Z. Zelazny, Phys. Scr. **T32**, 54 (1990).
[15] S. Cochavi, A. Moalem, D. Ashery, J. Alster, G. Bruge, and A. Chaumeaux, Nucl. Phys. **A211**, 21 (1973).
[16] M. Guttormsen, T. S. Tveter, L. Bergholt, F. Ingebretsen, and J. Rekstad, Nucl. Instrum. Methods Phys. Res. A **374**, 371 (1996).
[17] M. Guttormsen, T. Ramsøy, and J. Rekstad, Nucl. Instrum. Methods Phys. Res. A **255**, 518 (1987).
[18] D. M. Brink, Ph.D. thesis, Oxford University, 1955.
[19] P. Axel, Phys. Rev. **126**, 671 (1962).
[20] E. Ramakrishnan *et al.*, Phys. Lett. B **383**, 252 (2000).
[21] S. G. Kadmenskiĭ, V. P. Markushev, and V. I. Furman, Yad. Fiz. **37**, 277 (1983) [Sov. J. Nucl. Phys. **37**, 165 (1983)].
[22] V. K. Sirotkin, Yad. Fiz. **43**, 570 (1986) [Sov. J. Nucl. Phys. **43**, 362 (1986)].
[23] R. B. Firestone and V. S. Shirley, *Table of Isotopes*, 8th ed. (Wiley, New York, 1996), Vol. II.
[24] T. von Egidy, H. H. Schmidt, and A. N. Bekhami, Nucl. Phys. **A481**, 189 (1988).
[25] E. Tavukcu, Ph.D. thesis, North Carolina State University, 2002.
[26] R. Fischer, G. Traxler, M. Uhl, and H. Vonach, Phys. Rev. C **30**, 72 (1984).
[27] Masayuki Igashira, Hiroshi Matsumoto, Toshio Uchiyama, and Hideo Kitazawa, in *Proceedings of the International Conference on Nuclear Data for Science and Technology, Mito, Japan, 1988*, edited by S. Igarasi (Saikon, Tokyo, 1988), p. 67.
[28] P. E. Garrett, H. Lehmann, J. Jolie, C. A. McGrath, Minfang Yeh, W. Younes, and S. W. Yates, Phys. Rev. C **64**, 024316 (2001).
[29] E. Melby, L. Bergholt, M. Guttormsen, M. Hjorth-Jensen, F. Ingebretsen, S. Messelt, J. Rekstad, A. Schiller, S. Siem, and S. W. Ødegård, Phys. Rev. Lett. **83**, 3150 (1999).
[30] J. Dobaczewski, P. Magierski, W. Nazarewicz, W. Satuła, and Z. Szymański, Phys. Rev. C **63**, 024308 (2001).
[31] Mitsuo Sano and Shuichiro Yamasaki, Prog. Theor. Phys. **29**, 397 (1963).
[32] M. Guttormsen, A. Bjerve, M. Hjorth-Jensen, E. Melby, J. Rekstad, A. Schiller, S. Siem, and A. Belić, Phys. Rev. C **62**, 024306 (2000).
[33] K. K. Mon and J. B. French, Ann. Phys. (N.Y.) **95**, 90 (1975).